Anthracyclines Induce DNA Damage Response-Mediated Protection against Severe Sepsis

Nuno Figueiredo,[1,2,3,4,14] Angelo Chora,[1,14] Helena Raquel,[1,14] Nadja Pejanovic,[1] Pedro Pereira,[1] Björn Hartleben,[5] Ana Neves-Costa,[1] Catarina Moita,[1] Dora Pedroso,[1] Andreia Pinto,[1] Sofia Marques,[1] Hafeez Faridi,[6] Paulo Costa,[2] Raffaella Gozzelino,[7] Jimmy L. Zhao,[8] Miguel P. Soares,[7] Margarida Gama-Carvalho,[9] Jennifer Martinez,[10] Qingshuo Zhang,[11] Gerd Döring,[12,15] Markus Grompe,[11] J. Pedro Simas,[1] Tobias B. Huber,[5] David Baltimore,[8] Vineet Gupta,[6] Douglas R. Green,[10] João A. Ferreira,[1] and Luis F. Moita[1,13,*]

[1]Instituto de Medicina Molecular, Faculdade de Medicina, Universidade de Lisboa, 1649-028 Lisboa, Portugal
[2]Clínica Universitária de Cirurgia I, Centro Hospitalar Lisboa Norte, EPE, 1649-028 Lisboa, Portugal
[3]Gulbenkian Programme for Advanced Medical Education, 2780-156 Oeiras, Portugal
[4]Champalimaud Foundation, 1400-038 Lisboa, Portugal
[5]Renal Division, University Hospital Freiburg, 79106 Freiburg, Germany
[6]Department of Internal Medicine, Rush University Medical Center, Chicago, IL 60612, USA
[7]Instituto Gulbenkian de Ciência, Rua da Quinta Grande 6, 2780-156 Oeiras, Portugal
[8]Division of Biology, California Institute of Technology, Pasadena, CA 91125, USA
[9]Centro de Biodiversidade, Genómica Funcional e Integrativa (BioFIG), Faculdade de Ciências, Universidade de Lisboa, 1749-016 Lisboa, Portugal
[10]Department of Immunology, St Jude Children's Research Hospital, Memphis, TN 38105, USA
[11]Oregon Stem Cell Center, Department of Pediatrics, Oregon Health & Science University, Portland, OR 97239, USA
[12]Institut für Medizinische Mikrobiologie und Hygiene, University of Tübingen, 72076 Tübingen, Germany
[13]Clinical Research Center of The Lisbon Academic Medical Center, 1649-028 Lisboa, Portugal
[14]These authors contributed equally to this work
[15]Deceased July 2, 2013
*Correspondence: lmoita@fm.ul.pt
http://dx.doi.org/10.1016/j.immuni.2013.08.039

SUMMARY

Severe sepsis remains a poorly understood systemic inflammatory condition with high mortality rates and limited therapeutic options in addition to organ support measures. Here we show that the clinically approved group of anthracyclines acts therapeutically at a low dose regimen to confer robust protection against severe sepsis in mice. This salutary effect is strictly dependent on the activation of DNA damage response and autophagy pathways in the lung, as demonstrated by deletion of the ataxia telangiectasia mutated (*Atm*) or the autophagy-related protein 7 (*Atg7*) specifically in this organ. The protective effect of anthracyclines occurs irrespectively of pathogen burden, conferring disease tolerance to severe sepsis. These findings demonstrate that DNA damage responses, including the ATM and Fancony Anemia pathways, are important modulators of immune responses and might be exploited to confer protection to inflammation-driven conditions, including severe sepsis.

INTRODUCTION

Sepsis is a life-threatening condition that arises as a systemic inflammatory response to an infection (Bone et al., 1992; Levy et al., 2003). It includes a continuum of clinical severity ranging from systemic inflammatory response syndrome (SIRS), sepsis, severe sepsis, to septic shock (Suffredini and Munford, 2011). It is the leading cause of death in intensive care units and the third cause of overall hospital mortality (Angus and Wax, 2001; Ulloa and Tracey, 2005). In spite of substantial improvement in diagnosis and support measures, the global annual mortality rate is ~28% (Hotchkiss and Karl, 2003), ranging from less than 10% in SIRS to up to 70% in septic shock (Angus and Wax, 2001; Annane et al., 2003). The pathophysiology of sepsis remains poorly understood. As a result, the basic elements of treatment—early antibiotics, prompt control of the source of infection, and organ support—have not changed substantially in the last 50 years, and attempts to translate basic research results into effective new interventions have been met with limited or no success (Suffredini and Munford, 2011). In the same period, the incidence of sepsis and its economic burden has increased by 1% each year (Martin et al., 2003; Ulloa and Tracey, 2005), indicating the urgent need for novel therapeutic options.

Inflammation is a response to harmful stimuli that limits tissue damage and aims at restoring homeostasis (Medzhitov, 2008). Pathogen-associated molecular patterns (PAMPs) on microorganisms and damage-associated molecular patterns (DAMPs) originating from dying cells are sensed by the host through germline-encoded pattern-recognition receptors (PRRs) that recognize conserved signature structures in nonself and self (Janeway and Medzhitov, 2002). These sensors are present in both professional (including neutrophils, macrophages, and dendritic cells) and nonprofessional immune cells and their activation initiates intracellular signaling cascades leading to the transcriptional

CrossMark

expression of inflammatory mediators, such as cytokines and chemokines. Inflammation needs to be effectively terminated after removal of the original trigger for repair of damaged tissue to occur. In the susceptible host, overproduction of inflammatory mediators or an exaggerated response to their presence can lead to septic shock, tissue destruction, or permanent loss of function (Takeuchi and Akira, 2010).

There are two evolutionarily conserved defense strategies against infection that can limit host disease severity. One relies on reducing pathogen load, i.e., resistance to infection, whereas the other provides host tissue damage control, limiting disease severity irrespectively of pathogen load, i.e., tolerance to infection (Råberg et al., 2009; Schneider and Ayres, 2008). As demonstrated originally for plants and thereafter in *Drosophila*, tolerance to infection also operates in mammals, as revealed for *Plasmodium* (Råberg et al., 2007; Seixas et al., 2009) and polymicrobial infections in severe sepsis (Larsen et al., 2010).

Here we show in an experimental mouse model that anthracyclines confer strong protection against sepsis by increasing disease tolerance to infection; that is, acting irrespectively of pathogen burden. We further show that ATM (ataxia telangiectasia mutated) kinase and the induction of autophagy are strictly required for the in vivo protection against sepsis. These molecular pathways provide strong damage control in tissues, specifically in the lung.

RESULTS

Anthracyclines Confer Strong Protection against Severe Sepsis

In an in vitro chemical screen using ~2,320 compounds, we identified several lead candidates capable of inhibiting inflammatory cytokine production in response to *E. coli* challenge by the THP-1 macrophage line (see Figure S1A and Table S1 available online). This inhibitory effect was dissociated from cytotoxicity of the compounds tested on THP-1 cells (Figure S1B). Among these, we found three representatives of the anthracycline family of chemotherapeutic agents namely epirubicin, doxorubicin, and daunorubicin, and validated their inhibitory activity on cytokine production (Figure S1C).

We then used the cecal ligation and puncture (CLP) mouse model of experimental sepsis to investigate the in vivo effects of epirubicin (Rittirsch et al., 2009). In CLP, sepsis results from a polymicrobial infection of abdominal origin, leading to bacteremia and a systemic inflammatory response (Rittirsch et al., 2009). We adjusted CLP severity to a high-grade sepsis, where at least 80% of C57BL/6 mice succumbed within 48 hr after the initial procedure. Under these conditions, epirubicin administered intraperitoneally (i.p.) at the time of CLP and again 24 hr later in a total of 1.2 μg/g of body weight reproducibly and significantly ($p < 0.001$) increased the survival of C57BL/6 mice subjected to CLP by nearly 80%, without the use of antibiotics (Figure 1A). A similar protective effect was observed in epirubicin-treated animals with the same dose and schedule but administered i.v. (Figure S1D). This appeared to be a general property of the anthracycline family because other representative members of this family of drugs identified in the initial chemical screen conferred a similar degree of protection against CLP (Figure 1B). The protective effect of anthracyclines was not dependent on

the mouse strain as outbread NMRI mice were similarly protected by epirubicin (Figure 1C). Epirubicin was equally effective against another clinically relevant pathogen causing sepsis, *K. pneumoniae* administered intranasally (Figure 1D), arguing that epirubicin can be effective in the treatment of sepsis of different origins in addition to peritoneal sepsis. Mice previously subjected to CLP and treated with epirubicin were not immunocompromised because they could clear a secondary intranasal viral infection similarly to control mice (Figure 1E). Taken together, these results indicate that low doses of the anthracycline family of chemotherapeutic agents confer strong protection against severe sepsis, without causing host immunosuppression.

Epirubicin Acts Therapeutically to Promote Disease Tolerance to Severe Sepsis

We found that in epirubicin-treated mice subjected to CLP, the bacterial load in blood and target organs of sepsis, e.g., lung, liver, kidney, and spleen 24 hr post-CLP did not differ from that of untreated controls (Figure 2A). Although at 48 hr post-CLP, we noticed a trend toward a lower bacterial load in the target organs of epirubicin-treated animals, the differences were not statistically significant, even if most untreated control animals die between 24 and 48 hr after the CLP procedure. These results raised the possibility that the protective effect of epirubicin in vivo is related to disease tolerance without directly affecting the pathogen burden (Medzhitov et al., 2012). This idea was supported by the observation that the serum concentrations of several markers of tissue damage such as LDH (lung and general cellular damage), CK (muscle), ALT (liver), and urea (kidney) were substantially reduced to almost basal levels in epirubicin-treated mice, 24 hr after CLP, compared to untreated mice (Figure 2B). In addition, we observed a substantial reduction in the levels of inflammatory mediators including tumor necrosis factor (TNF), interleukin-1β (IL-1β), IL-6, and HMGB1 compared to nontreated CLP mice (Figure 2C). We have also observed improvement of histological lesions in the lung, liver, and kidney after CLP by treatment with epirubicin (Figure S2). To explore this further in the absence of bacteria, we found that the drug protected C57BL/6 mice from lethal septic shock caused by lipopolysaccharide (LPS, endotoxin) (Figure 2D).

Large spectrum antibiotics such as meropenem are very effective at lowering bacteremia and are standard drugs used in sepsis (Russell, 2006). We tested the efficacy of meropenem in CLP in comparison to epirubicin and found that although meropenem delayed the death rate of CLP-subjected mice, it did not prevent mortality (Figure 2E), in spite of a strong impact on bacterial burden (Figure 2F). This was in sharp contrast to the action of epirubicin, which did not interfere with bacteremia (Figure 2F) but prevented CLP-induced mortality (Figure 2E), again arguing for a role of epirubicin in conferring disease tolerance against severe sepsis (Larsen et al., 2010; Medzhitov et al., 2012).

Both epirubicin and meropenem decreased the amounts of IL-1β, TNF, and HMGB1 in the serum of mice subjected to CLP (Figure 2G). This indicates that whereas decreased circulating levels of inflammatory mediators might contribute to confer protection against severe sepsis, inhibition of IL-1β, TNF, and HMGB1 is not sufficient per se to explain the protective effect of epirubicin, which is in accordance with what is observed for other therapeutic approaches in the clinical setting (Hotchkiss and Karl, 2003).
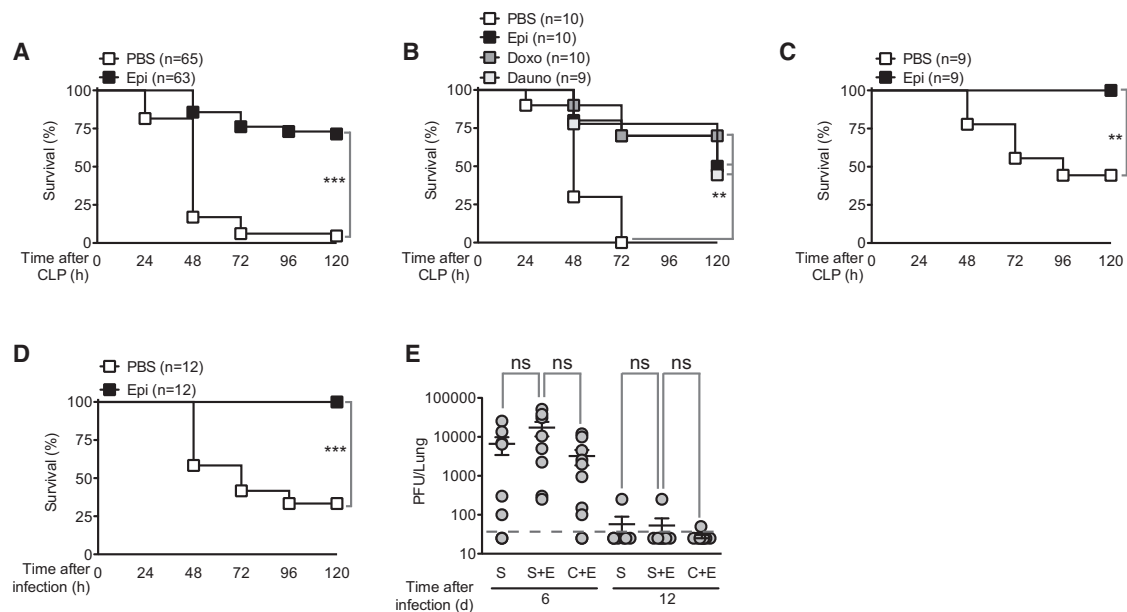
Figure 1. Epirubicin Affords Protection against Severe Sepsis

(A) Survival of C57BL/6 WT animals subjected to CLP treated with carrier (PBS) or epirubicin (Epi) (0.6 μg/g body weight) at the time of procedure and 24 hr later.

(B) Survival of C57BL/6 WT animals subjected to CLP treated with carrier (PBS), epirubicin (Epi), doxorubicin (Doxo), or daunorubicin (Dauno). Treatment schedule and doses as in (A).

(C) Survival of NMRI mice subjected to CLP and treated with carrier (PBS) or epirubicin (Epi) as in (A).

(D) Survival of C57BL/6 WT animals following intranasal inoculation of *Klebsiella pneumoniae* and treated with carrier (PBS) or epirubicin (Epi) as in (A).

(E) Quantification of infectious viral MuHV-4 particles in lung of C57BL/6 WT animals previously subjected to mock CLP (S), mock CLP treated with epirubicin (S+E) or CLP treated with epirubicin (C+E). Epirubicin treatment dose and schedule as in (A). Mice were intranasally inoculated with 1,000 PFU of MuHV-4 on day 3 post-CLP and viral particles quantified by plaque assay at days 6 and 12 after viral infection. Each circle represents individual animals and horizontal lines indicate arithmetic means ± SEM from two independent assays. The dashed horizontal line represents the limit of detection of the assay. n.s., not significant; *p < 0.05; **p < 0.01; ***p < 0.001 (log-rank [Mantel-Cox] test for A to D and Mann-Whitney test for E). See also Figure S1 and Table S1.

Taken together, these data suggest that epirubicin acts through an additional alternative mechanism to cytokine inhibition to confer tolerance to sepsis.

Epirubicin Protection against Sepsis Is Mediated by ATM

Next, in order to explore the molecular mechanism behind the protective effects of anthracyclines, we used our in vitro assay system to perform a short hairpin RNA (shRNA)-based screen in THP-1 cells, focusing on kinases and phosphatases and with IL-1β and TNF secretion as assay readouts. While our in vivo results suggested the possibility that anthracyclines ameliorate the lethal effects of sepsis by a mechanism affecting tissue tolerance, we reasoned that our in vitro assay would be useful for the identification of candidate pathways mediating the anthracycline effects. We found several negative regulators of IL-1β production in response to *E. coli* challenge, including the genes encoding ATM, checkpoint kinase 1 (CHEK1) and ataxia telangiectasia and Rad3 related (ATR) (Figure S3; Table S2). These findings suggest that DNA damage response (DDR) components are negative regulators of IL-1β secretion. By using a phospho-specific antibody against the activated form of ATM, we found that although *E. coli* alone was a poor but reproducible ATM activator (Figure S3), epirubicin alone or in combination with *E. coli* triggered a robust ATM activation (Figure S3). This was confirmed with immunoblotting (Figure S3).

ATM is a master regulator of the DDR (Ciccia and Elledge, 2010) and is known to be activated by anthracyclines and other DNA-damaging agents (Siu et al., 2004). Therefore, we used ATM-deficient mice to test the contribution of the DDR to the protective effect of anthracyclines against severe sepsis. ATM-deficient ($Atm^{-/-}$) mice were not protected by epirubicin against CLP and died with similar kinetics to those of wild-type (WT, $Atm^{+/+}$) animals that were treated with PBS alone (Figure 3A). We conclude that ATM expression is necessary to mediate the protective effect of epirubicin in sepsis. In striking contrast to WT mice (Figures 2B and 2C), in the absence of ATM, epirubicin no longer normalized the serologic markers of organ lesion (Figure 3B) or decreased the levels of inflammatory mediators (Figure 3C). However, in mice subjected to CLP and treated with etoposide (after in vivo titration to find the best and most effective dose), an agent known to cause DNA double-strand breaks and to activate ATM-dependent pathways (Montecucco and Biamonti, 2007), mortality induced by CLP was only partially rescued (Figure 3D), suggesting that ATM is necessary but not sufficient for the protection conferred by anthracyclines against sepsis.

In addition to double-strand breaks (repaired in an ATM-dependent manner), anthracyclines also cause DNA interstrand crosslinks, a DNA lesion known to be repaired by the Fanconi Anemia (FA) pathway (Ciccia and Elledge, 2010). Interestingly, FA patients were reported to spontaneously overproduce TNF (Briot et al., 2008; Vanderwerf et al., 2009), possibly because
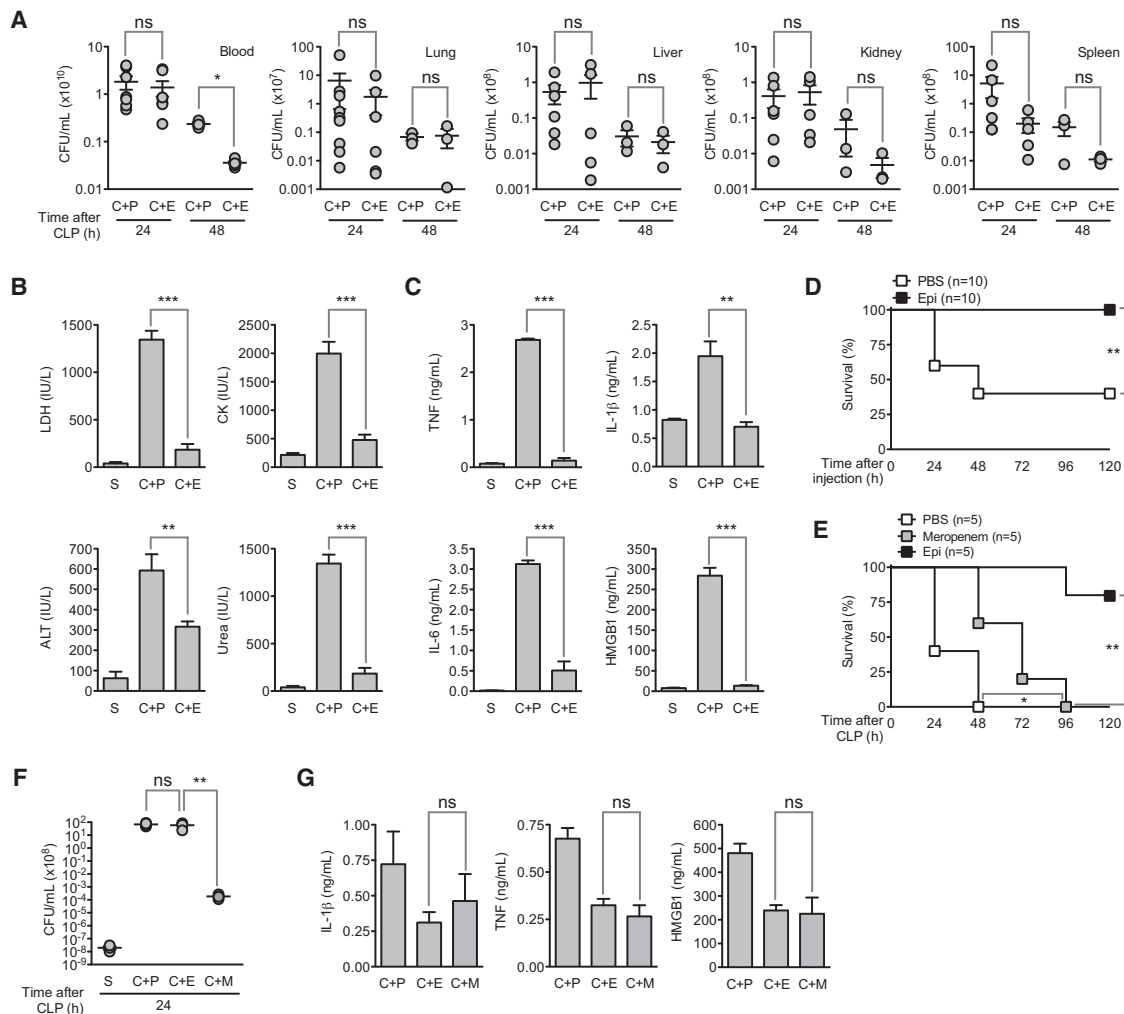
Figure 2. Epirubicin Promotes Disease Tolerance to Severe Sepsis

(A) Polymicrobial load (CFUs) in blood, lung, liver, kidney, and spleen, at indicated time points, of C57BL/6 animals undergoing CLP and treated with PBS (C+P) or epirubicin (C+E) (0.6 μg/g body weight) at the time of procedure and 24 hr later. Each circle represents individual animals. Horizontal lines indicate arithmetic means ± SEM.

(B) and (C) Epirubicin counteracts tissue damage and inflammation associated with CLP as assessed by (B) LDH, CK, ALT, urea, and (C) TNF, IL-1β, IL-6, and HMGB1 plasma concentrations in C57BL/6 WT animals 24 hr after mock CLP (S) (n = 2) or CLP followed by treatment with PBS (C+P) (n = 5) or epirubicin (C+E) (n = 7) as in (A). Results shown represent arithmetic means ± SEM from duplicate (B) or triplicate (C) readings per animal.

(D) Survival of C57BL/6 WT animals following lethal LPS injection and treatment with carrier (PBS) or epirubicin (Epi) as in (A).
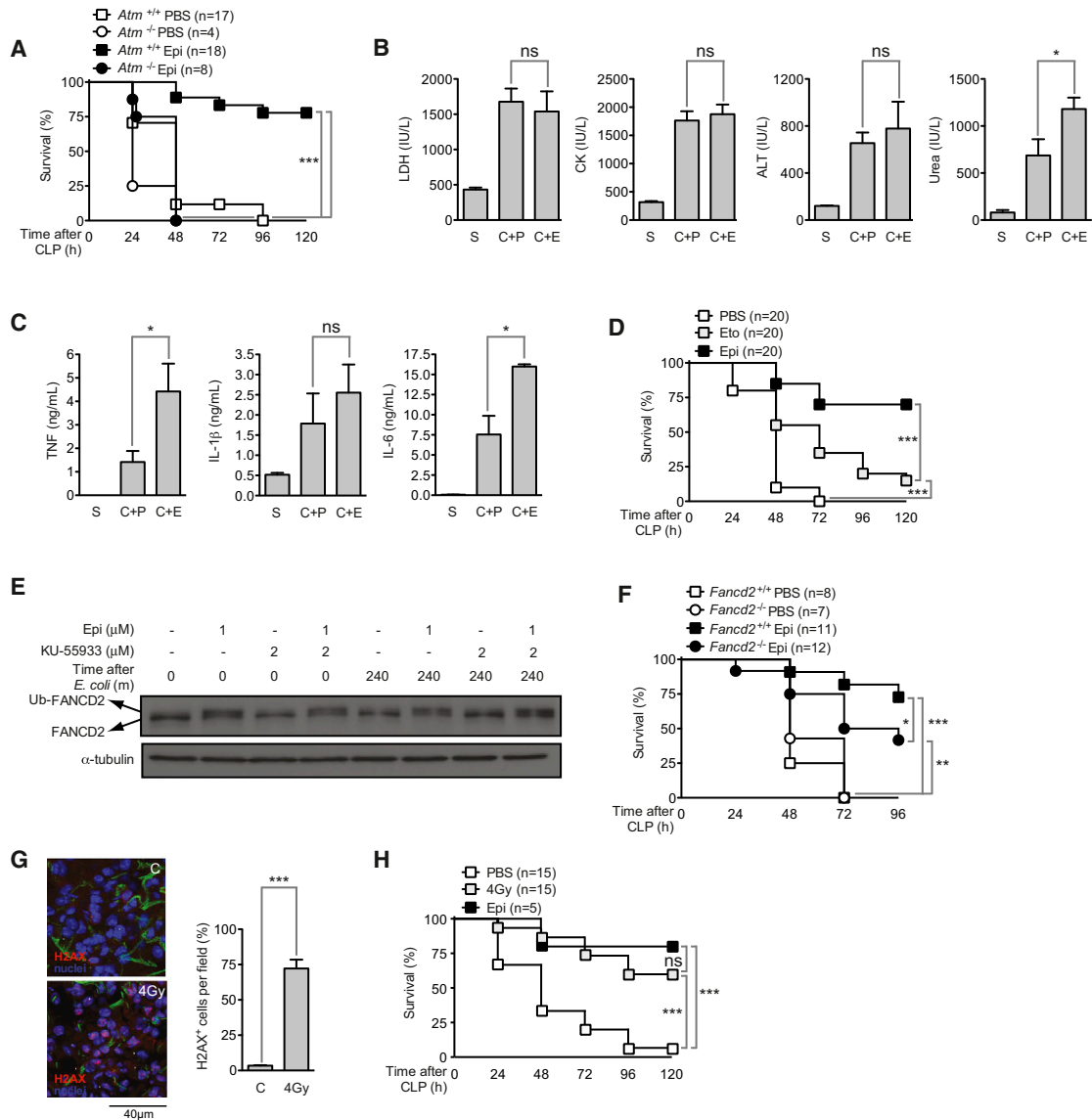
(E) Survival of C57BL/6 WT animals subjected to CLP treated with carrier (PBS), meropenem (40 μg/g body weight/day), or epirubicin (Epi) as in (A).

(F) CFUs in blood, at indicated time, of C57BL/6 animals undergoing mock CLP (S) or CLP followed by treatment with PBS (C+P), epirubicin (C+E), or meropenem (C+M) as in (A). Each circle represents individual animals. Horizontal lines indicate arithmetic means ± SEM.

(G) IL-1β, TNF, and HMGB1 plasma concentrations in C57BL/6 WT animals 24 hr after CLP followed by treatment with PBS (C+P) (n = 4), epirubicin (C+E) (n = 5), or meropenem (C+M) (n = 5) as in (C). n.s., not significant; *p < 0.05; **p < 0.01; ***p < 0.001 (log-rank [Mantel-Cox] test for D and E, Mann-Whitney test for A and F, and unpaired t test for B, C and G). See also Figure S2.

the FA protein FANCD2 can directly inhibit TNF promoter activity (Matsushita et al., 2011). In THP-1 cells, we observed that FANCD2 is activated in an ATM-independent manner upon epirubicin treatment, as shown by its monoubiquitination (Figure 3E). These findings support the independence of signaling events initiated by the generation of DNA double-strand breaks and DNA interstrand crosslinks. We examined the contribution of this pathway for epirubicin protection of CLP and found that *Fancd2*−/− mice were slightly but significantly (p < 0.05) impaired for the protective effects (Figure 3F).

These results suggest that activation of DDR is protective against sepsis. To further test this hypothesis, we have used whole-body sublethal γ irradiation. We found a significant increase in the number of cells with γH2AX-positive foci (p < 0.001), a surrogate marker of ATM activation (Ciccia and Elledge, 2010), in the lungs of whole-body sublethal γ-irradiated mice as compared to controls (Figure 3G). Mice subjected to CLP that were irradiated showed a significant increased survival (p < 0.001) as compared to nonirradiated mice (Figure 3H). We conclude that the protective phenotype induced

Figure 3. The Protection Afforded by Epirubicin against Severe Sepsis Is Mediated by ATM
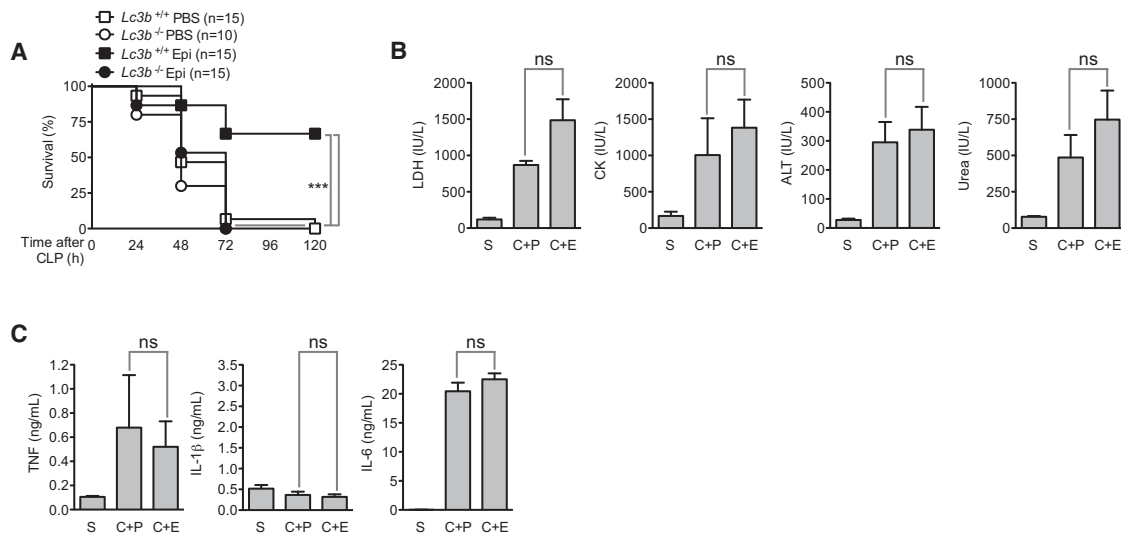
(A) Survival of $Atm^{+/+}$ and $Atm^{-/-}$ C57BL/6 animals subjected to CLP and treated with PBS or epirubicin (Epi) with same schedule and dose as in Figure 1.

(B) LDH, CK, ALT, urea, and (C) TNF, IL-1β, and IL-6 plasma concentrations in $Atm^{-/-}$ C57BL/6 animals 24 hr after mock CLP (S) (n = 2) or CLP followed by treatment with PBS (C+P) (n = 8) or epirubicin (C+E) (n = 8) as in (A). Results shown represent arithmetic means ± SEM from triplicate readings per animal.

(D) Survival of PBS-, etoposide (Eto)-, and epirubicin (Epi)-treated WT C57BL/6 animals undergoing CLP. Etoposide dose was 2 μg/g body weight. Treatment schedule is as in (A).

(E) FANCD2 and Ub-FANCD2 protein levels by immunoblotting in THP-1 cells following *E. coli* challenge after a preincubation (1 hr) with carrier, epirubicin, or KU-55933 as indicated.

(F) Survival of $Fancd2^{+/+}$ and $Fancd2^{-/-}$ animals subjected to CLP and treated with PBS or epirubicin (Epi) with same schedule and dose as in (A).

(G) Representative sections of γH2AX staining and percentage of γH2AX$^+$ cells per field (right panel) in lungs isolated 1 hr after mice were subjected to whole-body γ irradiation (4 Gy). Results shown represent arithmetic means ± SD from three fields.

(H) Survival of C57BL/6 WT animals subjected to CLP following whole-body γ irradiation (4Gy) or treated with carrier (PBS) or epirubicin (Epi) as in (A).

n.s., not significant; *p < 0.05; **p < 0.01; ***p < 0.001 (log-rank [Mantel-Cox] test for A, D, F and H and unpaired t test for B, C, and G). See also Figure S3 and Table S2.

by epirubicin is dependent on the activation of multiple pathways downstream of a DDR. The activation of the ATM pathway is the main contributor, but the full protection requires the activation of additional DDR pathways, including the FA pathway.

The Protective Effect of Epirubicin Is Dependent on the Autophagy Pathway

Although it is possible that the dominant ATM-mediated protection against sepsis might rely on ROS scavenging (Cosentino et al., 2011), on the induction of apoptosis of inflammatory cells

Figure 4. The ATM-Dependent Protection of Epirubicin against Severe Sepsis Relies on the Induction of Autophagy

(A) Survival of $Lc3b^{+/+}$ and $Lc3b^{-/-}$ animals subjected to CLP and treated with PBS or epirubicin (Epi) with same schedule and dose as in Figure 1.

(B) LDH, CK, ALT, urea, and (C) TNF, IL-1β, and IL-6 plasma concentrations in $Lc3b^{-/-}$ animals 24 hr after mock CLP (S) (n = 2) or CLP followed by treatment with PBS (C+P) (n = 4) or epirubicin (C+E) (n = 7) as in (2B). Results shown represent arithmetic means ± SEM from triplicate readings per animal. n.s., not significant; *p < 0.05; **p < 0.01; ***p < 0.001 (log-rank [Mantel-Cox] test for A, unpaired t test for B and C). See also Figure S4.

(Garrison et al., 2010), on the preservation of genomic stability (Westbrook and Schiestl, 2010), or on the biogenesis of anti-inflammatory microRNAs such as miR-146a (Zhang et al., 2011), we found no significant contribution for any of these processes (Figure S4). We therefore explored a possible role for autophagy in this process, given that ATM is a negative regulator of mTOR, which is an inhibitor of autophagy (Alexander et al., 2010a; Alexander et al., 2010b). By using autophagy-defective ($Lc3b^{-/-}$) mice, we found that the autophagy pathway is required for the in vivo effect of epirubicin (Figure 4A). Similarly to $Atm^{-/-}$ mice (Figures 3B and 3C), epirubicin was not able to decrease the serologic markers associated with organ lesion (Figure 4B) or to normalize cytokine levels in autophagy-defective mice (Figure 4C).

We then used LC3b-GFP mice to study the contribution of the autophagy pathway in the protection conferred by epirubicin. While FACS analysis shows that CLP alone induces LC3b aggregation in different splenocyte populations, namely monocytes and neutrophils, epirubicin treatment did not increase the autophagy pathway in these critical players in sepsis (Figure 5A). We then tested the impact of epirubicin on the survival of a conditional depletion of Atg7 specifically in neutrophils and monocytes upon CLP, with $Atg7^{loxP/loxP}$ $LysM^{Cre}$ GFP-LC3b animals. Strikingly, these animals were equally protected by epirubicin as compared to control mice (Figure 5B), suggesting that the autophagy pathway is not required in the myeloid compartment for the protective effects of epirubicin against sepsis.

Autophagy can be effectively monitored by the conversion and immobilization of LC3 (Kabeya et al., 2000). Because the autophagy pathway was not required in the myeloid compartment for protection against sepsis by epirubicin, we then looked at target organs of sepsis (lung, liver, and kidney) by using immunoblotting to identify lipidation of LC3b as indicative of activation of the autophagy pathway. We found that epirubicin specifically induced lipidation of LC3b in the lung at 6 hr, but not in the liver or kidney (Figure 5C). Although LC3 was transiently lipidated after CLP in the liver at 6 and 24 hr as previously reported (Chien et al., 2011), levels of LC3 were not altered by epirubicin treatment (Figure 5C). We have further confirmed that autophagy was induced in the lung as shown by the increase of LC3b positive vesicles in lung sections at 6 hr and 24 hr comparing epirubicin treated and nontreated mice (Figure 5D).

We then deleted Atg7 specifically in the lung (Figure S5) by using an adenovirus-expressing CRE (Ad^{cre}) to intranasally infect $Atg7^{loxP/loxP}$ mice (Komatsu et al., 2005). When subjected to CLP, these mice were no longer protected from CLP by epirubicin treatment (Figure 5E). In contrast to control mice, in $Atg7^{loxP/loxP}$ Ad^{cre} mice, the treatment with epirubicin does not improve the levels of circulating markers of organ lesion (Figure 5F). Accordingly, we observed a significant protective effect in survival after overexpression of ATG7 in the lung with adenovirus (Figure 5G).

By assessing the levels of γH2AX in the lungs of control or epirubicin-treated CLP-subjected mice, we found a significant increase in the number of cells with γH2AX-positive foci in lungs of epirubicin-treated mice (Figure 5H). To test whether ATM activation was also required in the lung, we used $Atm^{loxP/loxP}$ mice and Ad^{cre} to delete ATM specifically in the lung. Upon Ad^{cre}-mediated ATM deletion in the lung, mice were no longer protected against sepsis by treatment with epirubicin (Figure 5I). We therefore conclude that the protective effect of epirubicin in sepsis is, at least in part, dependent on the activation of ATM and of autophagy in target organs, namely the lung. These conclusions are further supported by intranasal delivery of epirubicin or etoposide to the lung (Figure 5J) because the protective effects as measured by survival are similar to the i.p. administration of those drugs (Figure 5J).
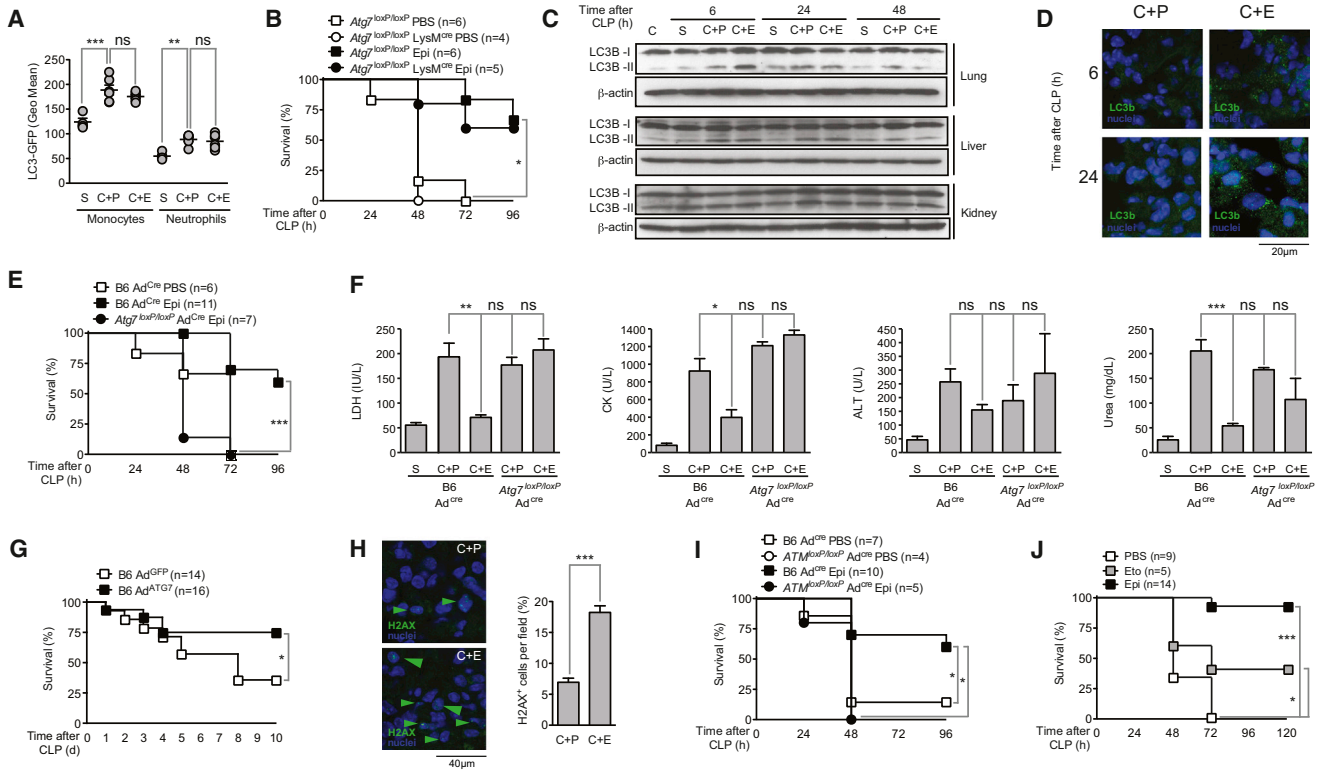
Figure 5. The Protective Effect of Epirubicin Is Dependent on the Activation of ATM and the Autophagy Pathway in the Lung

(A) GFP expression in blood monocytes and neutrophils, isolated from transgenic LC3b-GFP animals, 24 hr after mice were subjected to mock CLP (S) or CLP followed by treatment with PBS (C+P) or epirubicin (C+E) (0.6 μg/g body weight) at the time of procedure and 24 hr later. Each circle represents individual animals. Horizontal lines indicate arithmetic means ± SEM.

(B) Survival of $Atg7^{loxP/loxP}$ and $Atg7^{loxP/loxP}$ $LysM^{cre/cre}$ mice subjected to CLP and treated with PBS or epirubicin (Epi) with same schedule and dose as in (A).

(C) LC3B-I and LC3B-II protein levels by immunoblotting using a specific antibody against LC3B in lung, liver and kidney, isolated at the indicated times, of naive C57BL/6 animals (C) or mice subjected to mock CLP (S) or CLP followed by treatment with PBS (C+P) or epirubicin (C+E) as in (A).

(D) Representative sections of LC3b staining in lungs, isolated at the indicated times, of mice subjected to CLP followed by treatment with PBS (C+P) or epirubicin (C+E) as in (A).

(E) Survival of WT (B6) and $Atg7^{loxP/loxP}$ animals subjected to CLP and treated with PBS or epirubicin (Epi) with same schedule and dose as in (B) 5 days after inhalation of adenoviral vector encoding Cre (Ad^{Cre}).

(F) LDH, CK, ALT, and urea plasma concentrations in WT (B6 Ad^{Cre}) and $Atg7^{loxP/loxP}$ Ad^{Cre} animals 24 hr after mock CLP (S) (n = 2 for B6 Ad^{Cre}) or CLP followed by treatment with PBS (C+P) (n = 5 for B6 Ad^{Cre} and n = 2 for $Atg7^{loxP/loxP}$ Ad^{Cre}) or epirubicin (C+E) (n = 6 for B6 Ad^{Cre} and n = 3 for $Atg7^{loxP/loxP}$ Ad^{Cre}) as in (A).

(G) Survival of WT (B6) animals subjected to CLP 4 days after inhalation of adenoviral vector encoding GFP (Ad^{GFP}) or $Atg7$ (Ad^{ATG7}).

(H) Representative sections of γH2AX staining and percentage of γH2AX⁺ cells per field (right panel) in lungs, isolated 6 hr after mice were subjected to CLP followed by treatment with PBS (C+P) or epirubicin (C+E) as in (A). Results shown represent arithmetic means ± SD from ten fields.

(I) Survival of WT (B6) and $Atm^{loxP/loxP}$ animals subjected to CLP and treated with PBS or epirubicin (Epi) with same schedule and dose as in (B) 5 days after inhalation of Ad^{Cre}.

(J) Survival of C57BL/6 WT animals subjected to CLP treated with carrier (PBS), etoposide (2 μg/g body weight) or epirubicin (Epi) (0.6 μg/g body weight) intranasally, at the time of procedure and 24 hr later. n.s., not significant; *p < 0.05; **p < 0.01; ***p < 0.001 (log-rank [Mantel-Cox] test for B, E, G, I and J, Mann-Whitney test for A, and unpaired t test for F and H, right panel). See also Figure S5.

Epirubicin Has a 24 hr Therapeutic Window to Protect against Sepsis

Finally, we studied the therapeutic window of epirubicin in mice. When given alone, epirubicin conferred strong protection at the time of the procedure or until 3 hr after the initiation of CLP (Figure 6A). When administered only 6 hr after CLP, epirubicin quickly lost its protective effect (Figure 6A). However, if given in combination with meropenem, even when this antibiotic is only administered 12 hr after CLP, low-dose epirubicin conferred complete protection until at least 24 hr after the initial procedure (Figures 6B and 6C). These results suggest that anthracyclines

can be used not only to prevent sepsis but also that they can act therapeutically when their administration is combined with a large-spectrum antibiotic.

DISCUSSION

Here we report that epirubicin, and more generally the group of anthracyclines, are very effective at conferring protection against severe sepsis in mice, even when used up to 24 hr after the onset of infection. This therapeutic window is likely to be sufficient to make these drugs good candidates as useful therapeutic options
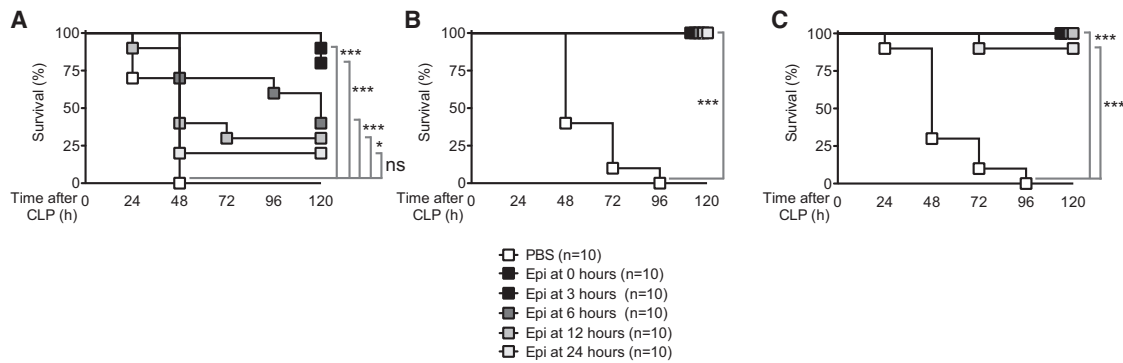
Figure 6. Epirubicin Confers Protection against Severe Sepsis in a Therapeutic Manner
(A) Survival of C57BL/6 WT animals subjected to CLP treated with PBS or epirubicin (same dose as in Figure 1) at indicated times in the absence of meropenem; (B) with administration of meropenem (40 μg/g body weight/day) starting at the time of the procedure or (C) with meropenem treatment starting 12 hr after CLP. n.s., not significant; *p < 0.05; **p < 0.01; ***p < 0.001 (log-rank [Mantel-Cox]).

in the clinic to reduce the mortality of sepsis in most patients that are either in the hospital or seek medical attention within the first few hours of symptoms initiation.

Although we began our investigation of the use of anthracyclines in sepsis by virtue of their effects in inhibiting inflammatory cytokine expression in myeloid cells in vitro, our studies have identified a mode of protection that seems to be much stronger and perhaps completely independent of such effects, and rather manifests at the level of DNA damage response and autophagy-induced protection in the lung. Thus, our findings uncover an unexpected role for these pathways in tissue (lung) tolerance to the pathological consequences of infection. These findings are especially relevant given that agents discovered in studies over the last few years targeting various proinflammatory cytokines have had limited success in humans. Our studies suggest a critical role for protecting host tissues thereby conferring protection against sepsis. Recent studies have highlighted the role of tissue tolerance to infection as an important aspect of host pathology (Medzhitov et al., 2012).

Interestingly, the protective effect of epirubicin seems to act irrespectively of the host pathogen burden, revealing that it confers disease tolerance to polymicrobial infection (Larsen et al., 2010; Råberg et al., 2009; Schneider and Ayres, 2008). This finding reveals that pharmacologic agents that provide tissue damage control can limit disease severity irrespectively of pathogen load and represent a promising therapeutic strategy against sepsis. Moreover, based on our identification of ATM as a major mediator of epirubicin effects, we propose that this protein and other components of the DNA damage response machinery constitute regulators of tolerance, without affecting pathogen resistance mechanisms.

Recent reports make our findings counterintuitive because doxorubicin and daunorubicin have been shown to induce acute inflammation when injected in the abdomen, where they induce cytokine secretion (Krysko et al., 2011; Sauter et al., 2011). However, the concentrations of anthracyclines utilized in these studies were more than 10-fold higher than those used here. By using lower concentrations, we might reduce the cytotoxicity of these drugs and the resulting release of proinflammatory DAMPs by dying cells and reveal the additional pharmacological effects mediated by the surviving target cells. Interestingly, fluo-

roquinolones that are bacterial type II topoisomerase inhibitors, as opposed to anthracyclines, which are eukaryotic type II topoisomerase inhibitors, were reported to have immunomodulatory effects (Dalhoff and Shalit, 2003) when used in supratherapeutic concentrations. Fluoroquinolones have been shown to protect against LPS model of septic shock (Khan et al., 2000). Although the molecular mechanisms that explain these effects have not been elucidated, it has been proposed that higher doses of fluoroquinolones can inhibit mammalian topoisomerase type II enzymes in addition to their bacterial targets (Dalhoff and Shalit, 2003), an effect that can be achieved with very low doses of anthracyclines.

The induction of autophagy is a common response to many forms of cellular stress, including DNA damage (Mizushima and Komatsu, 2011). The rationale for testing the role of autophagy was based on the knowledge that ATM is a negative regulator of mTOR and that mTOR is a negative regulator of autophagy (Alexander et al., 2010a; Alexander et al., 2010b). We therefore reasoned that if epirubicin activates ATM (as we have confirmed), then it is possible that it induces autophagy. This line of investigation made sense because several reports (Chien et al., 2011; Nakahira et al., 2011) have suggested a protective role for autophagy in sepsis. To probe the contribution of autophagy for the protective phenotype conferred by epirubicin, we have used two different genetic deletions in the autophagy pathway (LC3b and ATG7), and in both cases the protection normally conferred by epirubicin is lost. This is considered one of the best and most compelling ways to test the contribution of autophagy and the direction of autophagic flow (Klionsky et al., 2012).

Chien et al. have previously found that autophagy is transiently induced in the rat liver after CLP (Chien et al., 2011) and later made similar observations in the rat kidney (Hsiao et al., 2012). Chien et al. have speculated that the transient induction of autophagy in these organs could be required for protection and its decline at a later stage could contribute to the functional failure in liver during polymicrobial sepsis. After we found autophagy induction by epirubicin, we thought that one reason to explain anthracycline protection against CLP could be the sustained activation of autophagy in the liver and/or kidney preventing its decline as observed by Chien et al. Instead, we found that both in the liver and in the kidney, treatment with epirubicin did

not change this pattern, but instead transiently induced autophagy in the lung, a response that was not present in mice subjected to CLP in the absence of epirubicin treatment. We also report that epirubicin is highly protective when delivered directly to the lung and that overexpression of ATG7 specifically in the lung improves survival to CLP. Together, these observations strongly suggest that lung protection is critical and likely dominant because it prevents failure of additional organs, which makes our findings all the more relevant as the lung is the organ that often shows the first signs of dysfunction in septic patients and drives the failure of other target organs, particularly the kidney and later the liver (Hotchkiss and Karl, 2003).

Nakahira et al. demonstrate that depletion of the autophagic proteins LC3b and beclin 1 enhanced the activation of caspase-1 and secretion of IL-1β and IL-18 (Nakahira et al., 2011). Although we also observe inhibition of IL-1β secretion in vitro and in vivo by treatment with epirubicin, this finding is not dependent on the decreased activation of caspase-1 mediated by autophagy because even low concentrations of epirubicin lead to higher levels of active caspase-1 (A.C., data not shown), but this event is overshadowed by a strong inhibition of IL-1β, as well as most proinflammatory mediators that are NF-κB dependent, at the transcriptional level. We have now identified the mechanism: epirubicin targets the N-terminal region of p65, inhibiting transcription by blocking the DNA-binding ability of NF-κB (A.C., data not shown). The Nakahira et al. report also suggested to us that severe sepsis could cause DNA lesions capable of activating the inflammasome leading to chronic inflammation and that the induction of autophagy could block the inflammasome and prevent excessive inflammation. To address this possibility, we have used comet assays to look at different types of DNA damage in response to bacterial challenge in the presence and absence of epirubicin. We did find that *E. coli* alone triggers a small but measurable increase of DNA single-strand breaks (A.N.-C., data not shown). However, the presence of epirubicin does not decrease; rather, it increases DNA damage as compared to *E. coli* alone. Therefore, epirubicin does not decrease the generation of DNA-damaged species that can activate the inflammasome. We conclude that while the Nakahira et al. work clearly shows that autophagic proteins regulate NALP3-dependent inflammation by preserving mitochondrial integrity, the autophagy protection conferred by epirubicin to CLP does not depend on the mechanisms demonstrated in the Nakahira et al. (2011) paper, specifically the negative regulation of IL-1β secretion by autophagy.

Interestingly, the protective phenotype of epirubicin is strikingly similar to that of RIPK3-deficient mice (Duprez et al., 2011), suggesting that epirubicin-mediated, ATM-dependent autophagy induction can possibly prevent TNF-driven necroptosis in such key organs in sepsis pathology as the lung. In fact, there have been recent works that support the role of autophagy in the inhibition of necroptosis (Bray et al., 2012; Degenhardt et al., 2006; Lu and Walsh, 2012; Shen and Codogno, 2012), which could be achieved by targeting key necroptosis-signaling components (such as RIPK1 and RIPK3) for degradation. It is also possible that autophagy protects against severe sepsis because its activation increases the degradation of proinflammatory mediators with an important role in sepsis, like HMGB1 (Li et al., 2011). In addition, increased effective autophagy can

be beneficial in sepsis as a result of its critical role in the removal of damaged mitochondria in an ATM-dependent manner (Valentin-Vega and Kastan, 2012). The molecular mechanisms at the basis of epirubicin-induced protection in sepsis by autophagy are certainly an interesting topic for future studies.

EXPERIMENTAL PROCEDURES

Animal Model and Anthracycline Treatment

Animal care and experimental procedures were conducted in accordance with Portuguese and US guidelines and regulations after approval by the respective local committees (Instituto de Medicina Molecular and Instituto Gulbenkian de Ciência). All mice used were 8–12 weeks old. Mice were bred and maintained under specific pathogen-free (SPF) conditions. C57BL/6 and C57BL/6 $Atm^{-/-}$ mice were obtained from the Instituto Gulbenkian de Ciência (a kind gift from Dr. Vasco Barreto). C57BL/6 $Nrf2^{-/-}$ mice were provided originally from the RIKEN BioResource Center (Koyadai) and subsequently by the Instituto Gulbenkian de Ciência. LC3b$^{-/-}$ (B6129PF2/J background) and NMRI mice were purchased from Jackson and Charles River laboratories, respectively. miR-146a-deficient mice were generated in the Baltimore's laboratory (Boldin et al., 2011). $Fancd2^{-/-}$ mice were generated by the Grompe laboratory (Houghtaling et al., 2003). $Atg7^{loxP/loxP}$ were generated by Masaaki Komatsu and obtained from the Green laboratory. $Atm^{loxP/loxP}$ mice were generated and obtained from the F.W. Alt's laboratory. CLP was performed as described previously (Rittirsch et al., 2009). The endotoxemia model was performed by injecting i.p. a single dose of 50 μg/g body weight of LPS (from *E. coli* serotype 026:B6; Sigma-Aldrich). Pulmonary monostrain infections were carried out as described previously (Weber et al., 2011), with intranasal injection of *Klebsiella pneumoniae* (ATCC13803) at 8 × 10^7 colony-forming units (CFUs). Epirubicin (Sigma-Aldrich), doxorubicin (Sigma-Aldrich), and daunorubicin (Sigma-Aldrich) and meropenem (AstraZeneca) were dissolved in PBS, and etoposide (Sigma-Aldrich) was dissolved in DMSO, aliquoted, and stored at −80°C. Epirubicin and daunorubicin (0.6 μg/g body weight), doxorubicin (0.5 μg/g body weight), and etoposide (2 μg/g body weight) were injected i.p. at 0 and 24 hr following CLP. Meropenem (20 μg/g body weight b.i.d.) was injected i.p. for 5 consecutive days.

Colony-Forming Units Assay

Blood samples from septic or mock CLP mice were collected by cardiac puncture at indicated times after surgery. Mice were subsequentially perfused in toto with 10 mL ice cold PBS and spleen, liver, and kidneys were surgically removed and homogenized in 5 mL of sterile PBS. Serial dilutions of blood and tissue homogenates were immediately plated on Trypticase Soy Agar II plates supplemented with 5% Sheep Blood. CFUs were counted after a 12 hr incubation at 37°C.

Serology and Cytokine Measurement

Plasma from blood samples obtained 24 hr post-CLP was collected after centrifugation. LDH, CK, ALT, and urea levels were measured with the BioAssay Systems kits (BioAssay Systems) according to company's protocol. Levels of TNF, IL-1β, and IL-6 were measured with the murine ELISA kits (R&D Systems) according to company's protocol. Levels of HMGB1 were assessed with a murine ELISA kit (Shino Test Corporation) according to company's protocol.

Histology

Mice were euthanized and perfused in toto with 10 mL ice cold PBS, and lungs and livers were surgically removed. Livers were placed in 10% phosphate buffered formalin for 24 hr after which they were embedded in paraffin. Sections were subsequently incubated with a primary antibody reactive to HMGB1 (Abcam) followed by incubation with biotinylated secondary antibody and then with biotinylated horseradish peroxidase. Staining was developed by addition of diaminobenzidine (DAB) substrate (Vector Labs) and counterstained with hematoxylin. Lungs were embedded in Tissue-Tek OCT (Sakura) and snap frozen in liquid nitrogen. Lung sections (7 μm) were fixed in 1% paraformaldehyde in PBS for 2 min, followed by methanol at −20°C for 10 min and then in acetone for 2 min. Detection of LC3b and histone γH2AX

was performed by incubating sections overnight at 4°C with rabbit polyclonal antibodies specific for, respectively, LC3b (L7543, Sigma Aldrich) and γH2AX (phosphoS139; ab2893; Abcam); incubation with a secondary DyLight 488-coupled antibody (Jackson ImmunoResearch Laboratories) was for 1 hr at room temperature. Sections were counterstained with DAPI (0.5 μg/mL) to visualize DNA and mounted in Vectashield (Vector Laboratories) before confocal microscopy. Samples were examined with a Zeiss LSM 510 META laser scanning confocal microscope (Carl Zeiss). The acquired images were analyzed with a MATLAB (Mathworks) routine developed in-house to perform automatic threshold segmentation and enumeration of individual cell nuclei stained with DAPI.

In Vivo Viral Infection and Viral Titer Assay

Murid herpesvirus-4 infection and viral particle quantification was performed as previously described (Marques et al., 2008). Briefly, mice were intranasally inoculated with 1,000 PFU of MuHV-4 strain 68 in 20 μl of PBS under light iso-flurane anesthesia. At 6 and 12 days postinfection, lungs were removed and homogenized in 5 mL of Glasgow's modified Eagle's medium (GMEM). Infectious virus titers in freeze-thawed lung homogenates were determined by serial diluted suspension assay with Baby hamster kidney cells (BHK-21) cultured in GMEM supplemented with 10% fetal bovine serum, 10% tryptose phosphate broth, 2 mM glutamine, 100 U/ml penicillin, and 100 μg/ml streptomycin (GMEM). Plates were incubated for 4 days, fixed with 10% formal saline, and counterstained with toluidine blue. Viral plaques were counted with a plate microscope. Cre-adenovirus were obtained from the University of Iowa, prepared as a calcium-phosphate coprecipitate, and incubated for 20 min at room temperature. Atg7$^{loxP/loxP}$ and ATM$^{loxP/loxP}$ were subjected to light iso-flurane anesthesia and allowed to inhale 125 μL of virus at a concentration of 2.5 × 10^7 PFU. Additionally, WT C57BL/6 mice were included as controls. Mice were allowed to rest for 5 days after inhalation, after which they were subjected to CLP.

Stainings and Flow Cytometry

Peritoneal infiltrating leukocytes from either WT or LC3b-GFP transgenic animals were obtained 24 hr post CLP by lavage with 5 mL of sterile ice-cold PBS, washed, and blocked with mouse Ab anti-FcγIII/II (clone 93) receptor diluted in PBS containing 2% FCS (v/v) for 20 min at 4°C. Surface markers were detected by incubating for 30 min at 4°C with mouse Ab anti-CD4 (clone GK1.5), anti-CD8 (clone 53-6.7), anti-CD19 (clone 6D5), anti-Ly-6G (clone 1A8) (all Biolegend), and anti-neutrophil monoclonal antibody (clone 7/4) (Abcam). Dead cells were excluded by costaining with propidium iodide. Total cell number was determined by flow cytometry with a fixed number of latex beads (Beckman Coulter) coacquired with a pre-established volume of the cellular suspension. For phospho-ATM intracellular staining, stimulated THP-1 cells were washed and fixed with ice-cold methanol. Mouse Ab anti-phospho-ATM pS1981, clone 10H11.E12 (IgG1k) was incubated for 60 min at room temperature followed by an incubation of secondary Ab conjugated with Alexa 488 (Molecular Probes). Fluorescence was measured by flow cytometry and data analyzed with FlowJo software.

Immunoblotting

Mouse phospho-ATM (4526, Cell Signaling, 1:1,000 dilution), rabbit total ATM (2873, Cell Signaling, 1:1000 dilution), rabbit LC3b (Sigma, 1:1000 dilution) and the rabbit Fancd2 (Novus Biologicals; 1:1000 dilution) Ab were used overnight at 4°C. Primary Ab were detected with peroxidase conjugated secondary Ab (1 hr; RT) and developed with SuperSignal chemiluminescent detection kit (Pierce).

SUPPLEMENTAL INFORMATION

Supplemental Information includes five figures, two tables, and Supplemental Experimental Procedures and can be found with this article online at http://dx.doi.org/10.1016/j.immuni.2013.08.039.

ACKNOWLEDGMENTS

We are grateful to Vasco Barreto for Atm$^{-/-}$ and Frederick Alt for Atm$^{loxP/loxP}$ mice. We thank Mario Ramirez for bacterial strains to probe epirubicin protec-

REFERENCES

Alexander, A., Cai, S.L., Kim, J., Nanez, A., Sahin, M., MacLean, K.H., Inoki, K., Guan, K.L., Shen, J., Person, M.D., et al. (2010a). ATM signals to TSC2 in the cytoplasm to regulate mTORC1 in response to ROS. Proc. Natl. Acad. Sci. USA 107, 4153–4158.

Alexander, A., Kim, J., and Walker, C.L. (2010b). ATM engages the TSC2/mTORC1 signaling node to regulate autophagy. Autophagy 6, 672–673.

Angus, D.C., and Wax, R.S. (2001). Epidemiology of sepsis: an update. Crit. Care Med. Suppl. 29, S109–S116.

Annane, D., Aegerter, P., Jars-Guincestre, M.C., and Guidet, B.; CUB-Réa Network. (2003). Current epidemiology of septic shock: the CUB-Réa Network. Am. J. Respir. Crit. Care Med. 168, 165–172.

Boldin, M.P., Taganov, K.D., Rao, D.S., Yang, L., Zhao, J.L., Kalwani, M., Garcia-Flores, Y., Luong, M., Devrekanli, A., Xu, J., et al. (2011). miR-146a is a significant brake on autoimmunity, myeloproliferation, and cancer in mice. J. Exp. Med. 208, 1189–1201.

Bone, R.C., Sibbald, W.J., and Sprung, C.L. (1992). The ACCP-SCCM consensus conference on sepsis and organ failure. Chest 101, 1481–1483.

Bray, K., Mathew, R., Lau, A., Kamphorst, J.J., Fan, J., Chen, J., Chen, H.Y., Ghavami, A., Stein, M., DiPaola, R.S., et al. (2012). Autophagy suppresses RIP kinase-dependent necrosis enabling survival to mTOR inhibition. PLoS ONE 7, e41831.

Briot, D., Macé-Aimé, G., Subra, F., and Rosselli, F. (2008). Aberrant activation of stress-response pathways leads to TNF-alpha oversecretion in Fanconi anemia. Blood 111, 1913–1923.

Chien, W.S., Chen, Y.H., Chiang, P.C., Hsiao, H.W., Chuang, S.M., Lue, S.I., and Hsu, C. (2011). Suppression of autophagy in rat liver at late stage of polymicrobial sepsis. Shock 35, 506–511.

Ciccia, A., and Elledge, S.J. (2010). The DNA damage response: making it safe to play with knives. Mol. Cell 40, 179–204.

Cosentino, C., Grieco, D., and Costanzo, V. (2011). ATM activates the pentose phosphate pathway promoting anti-oxidant defence and DNA repair. EMBO J. 30, 546–555.

Dalhoff, A., and Shalit, I. (2003). Immunomodulatory effects of quinolones. Lancet Infect. Dis. 3, 359–371.

Degenhardt, K., Mathew, R., Beaudoin, B., Bray, K., Anderson, D., Chen, G., Mukherjee, C., Shi, Y., Gélinas, C., Fan, Y., et al. (2006). Autophagy promotes tumor cell survival and restricts necrosis, inflammation, and tumorigenesis. Cancer Cell 10, 51–64.

Duprez, L., Takahashi, N., Van Hauwermeiren, F., Vandendriessche, B., Goossens, V., Vanden Berghe, T., Declercq, W., Libert, C., Cauwels, A., and Vandenabeele, P. (2011). RIP kinase-dependent necrosis drives lethal systemic inflammatory response syndrome. Immunity 35, 908–918.

Garrison, S.P., Thornton, J.A., Häcker, H., Webby, R., Rehg, J.E., Parganas, E., Zambetti, G.P., and Tuomanen, E.I. (2010). The p53-target gene puma drives neutrophil-mediated protection against lethal bacterial sepsis. PLoS Pathog. 6, e1001240.

Hotchkiss, R.S., and Karl, I.E. (2003). The pathophysiology and treatment of sepsis. N. Engl. J. Med. 348, 138–150.

Houghtaling, S., Timmers, C., Noll, M., Finegold, M.J., Jones, S.N., Meyn, M.S., and Grompe, M. (2003). Epithelial cancer in Fanconi anemia

complementation group D2 (Fancd2) knockout mice. Genes Dev. 17, 2021–2035.

Hsiao, H.W., Tsai, K.L., Wang, L.F., Chen, Y.H., Chiang, P.C., Chuang, S.M., and Hsu, C. (2012). The decline of autophagy contributes to proximal tubular dysfunction during sepsis. Shock 37, 289–296.

Janeway, C.A., Jr., and Medzhitov, R. (2002). Innate immune recognition. Annu. Rev. Immunol. 20, 197–216.

Kabeya, Y., Mizushima, N., Ueno, T., Yamamoto, A., Kirisako, T., Noda, T., Kominami, E., Ohsumi, Y., and Yoshimori, T. (2000). LC3, a mammalian homologue of yeast Apg8p, is localized in autophagosome membranes after processing. EMBO J. 19, 5720–5728.

Khan, A.A., Slifer, T.R., Araujo, F.G., Suzuki, Y., and Remington, J.S. (2000). Protection against lipopolysaccharide-induced death by fluoroquinolones. Antimicrob. Agents Chemother. 44, 3169–3173.

Klionsky, D.J., Abdalla, F.C., Abeliovich, H., Abraham, R.T., Acevedo-Arozena, A., Adeli, K., Agholme, L., Agnello, M., Agostinis, P., Aguirre-Ghiso, J.A., et al. (2012). Guidelines for the use and interpretation of assays for monitoring autophagy. Autophagy 8, 445–544.

Komatsu, M., Waguri, S., Ueno, T., Iwata, J., Murata, S., Tanida, I., Ezaki, J., Mizushima, N., Ohsumi, Y., Uchiyama, Y., et al. (2005). Impairment of starvation-induced and constitutive autophagy in Atg7-deficient mice. J. Cell Biol. 169, 425–434.

Krysko, D.V., Kaczmarek, A., Krysko, O., Heyndrickx, L., Woznicki, J., Bogaert, P., Cauwels, A., Takahashi, N., Magez, S., Bachert, C., and Vandenabeele, P. (2011). TLR-2 and TLR-9 are sensors of apoptosis in a mouse model of doxorubicin-induced acute inflammation. Cell Death Differ. 18, 1316–1325.

Larsen, R., Gozzelino, R., Jeney, V., Tokaji, L., Bozza, F.A., Japiassú, A.M., Bonaparte, D., Cavalcante, M.M., Chora, A., Ferreira, A., et al. (2010). A central role for free heme in the pathogenesis of severe sepsis. Sci. Transl. Med. 2, 51ra71.

Levy, M.M., Fink, M.P., Marshall, J.C., Abraham, E., Angus, D., Cook, D., Cohen, J., Opal, S.M., Vincent, J.L., and Ramsay, G.; SCCM/ESICM/ACCP/ATS/SIS. (2003). 2001 SCCM/ESICM/ACCP/ATS/SIS International Sepsis Definitions Conference. Crit. Care Med. 31, 1250–1256.

Li, W., Zhu, S., Li, J., Assa, A., Jundoria, A., Xu, J., Fan, S., Eissa, N.T., Tracey, K.J., Sama, A.E., and Wang, H. (2011). EGCG stimulates autophagy and reduces cytoplasmic HMGB1 levels in endotoxin-stimulated macrophages. Biochem. Pharmacol. 81, 1152–1163.

Lu, J.V., and Walsh, C.M. (2012). Programmed necrosis and autophagy in immune function. Immunol. Rev. 249, 205–217.

Marques, S., Alenquer, M., Stevenson, P.G., and Simas, J.P. (2008). A single CD8+ T cell epitope sets the long-term latent load of a murid herpesvirus. PLoS Pathog. 4, e1000177.

Martin, G.S., Mannino, D.M., Eaton, S., and Moss, M. (2003). The epidemiology of sepsis in the United States from 1979 through 2000. N. Engl. J. Med. 348, 1546–1554.

Matsushita, N., Endo, Y., Sato, K., Kurumizaka, H., Yamashita, T., Takata, M., and Yanagi, S. (2011). Direct inhibition of TNF-α promoter activity by Fanconi anemia protein FANCD2. PLoS ONE 6, e23324.

Medzhitov, R. (2008). Origin and physiological roles of inflammation. Nature 454, 428–435.

Medzhitov, R., Schneider, D.S., and Soares, M.P. (2012). Disease tolerance as a defense strategy. Science 335, 936–941.

Mizushima, N., and Komatsu, M. (2011). Autophagy: renovation of cells and tissues. Cell 147, 728–741.

Montecucco, A., and Biamonti, G. (2007). Cellular response to etoposide treatment. Cancer Lett. 252, 9–18.

Nakahira, K., Haspel, J.A., Rathinam, V.A., Lee, S.J., Dolinay, T., Lam, H.C., Englert, J.A., Rabinovitch, M., Cernadas, M., Kim, H.P., et al. (2011). Autophagy proteins regulate innate immune responses by inhibiting the release of mitochondrial DNA mediated by the NALP3 inflammasome. Nat. Immunol. 12, 222–230.

Råberg, L., Sim, D., and Read, A.F. (2007). Disentangling genetic variation for resistance and tolerance to infectious diseases in animals. Science 318, 812–814.

Råberg, L., Graham, A.L., and Read, A.F. (2009). Decomposing health: tolerance and resistance to parasites in animals. Philos. Trans. R. Soc. Lond. B Biol. Sci. 364, 37–49.

Rittirsch, D., Huber-Lang, M.S., Flierl, M.A., and Ward, P.A. (2009). Immunodesign of experimental sepsis by cecal ligation and puncture. Nat. Protoc. 4, 31–36.

Russell, J.A. (2006). Management of sepsis. N. Engl. J. Med. 355, 1699–1713.

Sauter, K.A., Wood, L.J., Wong, J., Iordanov, M., and Magun, B.E. (2011). Doxorubicin and daunorubicin induce processing and release of interleukin-1β through activation of the NLRP3 inflammasome. Cancer Biol. Ther. 11, 1008–1016.

Schneider, D.S., and Ayres, J.S. (2008). Two ways to survive infection: what resistance and tolerance can teach us about treating infectious diseases. Nat. Rev. Immunol. 8, 889–895.

Seixas, E., Gozzelino, R., Chora, A., Ferreira, A., Silva, G., Larsen, R., Rebelo, S., Penido, C., Smith, N.R., Coutinho, A., and Soares, M.P. (2009). Heme oxygenase-1 affords protection against noncerebral forms of severe malaria. Proc. Natl. Acad. Sci. USA 106, 15837–15842.

Shen, H.M., and Codogno, P. (2012). Autophagy is a survival force via suppression of necrotic cell death. Exp. Cell Res. 318, 1304–1308.

Siu, W.Y., Lau, A., Arooz, T., Chow, J.P., Ho, H.T., and Poon, R.Y. (2004). Topoisomerase poisons differentially activate DNA damage checkpoints through ataxia-telangiectasia mutated-dependent and -independent mechanisms. Mol. Cancer Ther. 3, 621–632.

Suffredini, A.F., and Munford, R.S. (2011). Novel therapies for septic shock over the past 4 decades. JAMA 306, 194–199.

Takeuchi, O., and Akira, S. (2010). Pattern recognition receptors and inflammation. Cell 140, 805–820.

Ulloa, L., and Tracey, K.J. (2005). The "cytokine profile": a code for sepsis. Trends Mol. Med. 11, 56–63.

Valentin-Vega, Y.A., and Kastan, M.B. (2012). A new role for ATM: regulating mitochondrial function and mitophagy. Autophagy 8, 840–841.

Vanderwerf, S.M., Svahn, J., Olson, S., Rathbun, R.K., Harrington, C., Yates, J., Keeble, W., Anderson, D.C., Anur, P., Pereira, N.F., et al. (2009). TLR8-dependent TNF-(alpha) overexpression in Fanconi anemia group C cells. Blood 114, 5290–5298.

Weber, S.E., Tian, H., and Pirofski, L.A. (2011). CD8+ cells enhance resistance to pulmonary serotype 3 Streptococcus pneumoniae infection in mice. J. Immunol. 186, 432–442.

Westbrook, A.M., and Schiestl, R.H. (2010). Atm-deficient mice exhibit increased sensitivity to dextran sulfate sodium-induced colitis characterized by elevated DNA damage and persistent immune activation. Cancer Res. 70, 1875–1884.

Zhang, X., Wan, G., Berger, F.G., He, X., and Lu, X. (2011). The ATM kinase induces microRNA biogenesis in the DNA damage response. Mol. Cell 41, 371–383.